On the nature of dense CO adlayers on fcc(100) surfaces: a kinetic Monte Carlo study

C. G. M. Hermse, M. M. M. Jansen, A. P. van Bavel, J. J. Lukkien, R. A. van Santen and A. P. J. Jansen

Received 12th June 2009, Accepted 13th October 2009
First published as an Advance Article on the web 12th November 2009
DOI: 10.1039/b911322c

We present a kinetic Monte Carlo lattice gas model including top and bridge sites on a square lattice, with pairwise lateral interactions between the adsorbates. In addition to the pairwise lateral interactions we include an additional interaction: an adsorbate is forbidden to adsorb on a bridge site formed by two surface atoms when both surface atoms are already forming a bond with an adsorbate. This model is used to reproduce the low and high coverage adsorption behaviour of CO on Pt(100) and Rh(100). The parameter set used to simulate CO on Pt(100) produces the c(2 × 2)–2t ordered structure at 0.50 ML coverage, a one-dimensionally ordered structure similar to the experimentally observed $(3\sqrt{2} \times \sqrt{2}) - 2t + 2b$ structure at 0.67 ML coverage, the c(4 × 2)−4t + 2b ordered structure at 0.75 ML coverage, and the recently reported c(6 × 2)−6t + 4b ordered structure at 0.83 ML coverage. The $(5\sqrt{2} \times \sqrt{2})$ ordered structure at 0.60 ML coverage is not reproduced by our model. The parameter set used to simulate CO on Rh(100) produces the c(2 × 2)−2t ordered structure at 0.50 ML coverage, a one-dimensionally ordered structure similar to the experimentally observed $(4\sqrt{2} \times \sqrt{2}) - 2t + 4b$ structure at 0.75 ML coverage, and the c(6 × 2)−6t + 4b ordered structure at 0.83 ML coverage. Additionally, the simulated change of top and bridge site occupation as a function of coverage matches the trend in experimental vibrational peak intensities.

1. Introduction

Ordered adlayer structures for CO on fcc(100) surfaces of transition metals are long-established. The real space structures are in general derived from low energy electron diffraction (LEED) measurements back in the eighties. The information from these LEED patterns combined with the estimated coverage from adsorption isotherms have been used to construct possible real space structures. Unit cell sizes could be determined. An educated guess could then be made about the distribution of adsorbates inside the unit cell, keeping in mind that adsorbates in general tend to keep as far apart as possible. The positions of the adsorbates within the unit cell could be obtained by dynamical LEED I/V-analyses.[1–3]

Further vibrational spectroscopy measurements allowed the distinction between bridge and top bound CO on the surface. This caused the proposed ordered structures to be confirmed or further refined. In some cases, however, there were problems related to the fact that the vibrational intensities do not reflect the actual abundance of a species, and in other cases binding site assignments based on the vibrational frequency had to be reconsidered.[1–6] Finally this resulted in a set of common, well accepted ordered structures for CO adsorption on transition metals like platinum, rhodium, nickel, copper and palladium. These include a $c(2\sqrt{2} \times \sqrt{2})$ and a c(2 × 2) structure at half a monolayer (0.50 ML) coverage, a $c(5\sqrt{2} \times \sqrt{2})$ structure at 0.60 ML, a $(3\sqrt{2} \times \sqrt{2})$ structure at 0.67 ML, a c(4 × 2) or $(4\sqrt{2} \times \sqrt{2})$ structure at 0.75 ML, and a "split" (2 × 1) or c(6 × 2) at 0.83 ML coverage.[7–13]

There is a catch here, though. CO adsorbs on both top and bridge sites on platinum and rhodium (on copper only top sites, and on palladium only bridge sites are occupied). This means that, with three surface sites (one top and two bridge) available per surface atom, and a unit cell area of four to twelve surface atoms (depending on the ordered structure), there are many possible ways to distribute the adsorbates inside the unit cell. Some of these would clearly not make sense at all, but several others can be thought of as reasonable at first sight. Which adsorbate distribution is actually present can not be derived from standard LEED experiments and vibrational spectroscopy measurements alone (though a combination of LEED-IV and calculations is still an option). Candidate techniques to resolve this problem are scanning tunneling microscopy (STM), electronic structure calculations (for example DFT), and lattice gas modelling. STM can reach atomic resolution, and can therefore in principle be used to determine the exact position of each adsorbate inside the unit cell. A complicating factor is that in STM images sometimes not all adsorbates are visible. For example, for NO on Rh(111) it has been demonstrated that in ordered structures with both top and threefold bound adsorbates, only the top bound adsorbates are detected by the STM tip.[14] Furthermore, CO is in general difficult to image in STM due to its high mobility. The interaction with the STM tip may cause the CO molecules

Schuit Institute of Catalysis, ST/SKA, Eindhoven University of Technology, P. O. Box 513, 5600 MB Eindhoven, The Netherlands. E-mail: chretien@sg10.chem.tue.nl, a.p.j.jansen@tue.nl

to switch site, or the molecules may move spontaneously from one site to another during the time span that is required to record a full STM image. To the best of our knowledge, only one STM study into the high coverage ordered structures of CO on fcc(100) surfaces has been reported.[15]

Another approach is to use the knowledge regarding the size of the unit cell in a DFT calculation. One could do a simulation with the unit cell size as determined by LEED, and systematically place a specified number of adsorbates on the various accessible sites within the unit cell. The structure with the highest adsorption energy would then be the one most likely to be found in practice. There are also drawbacks to this approach, however. On one hand, the difference in adsorption energy between various ordered structures can be very small. The entropic contribution to the stability of each ordered structure is not accounted for in standard DFT calculations: this is because DFT calculations considers only few unit cells, while an actual adlayer is built up of many unit cells and can therefore show more than one type of unit cell, rotationally equivalent domains, phase boundaries and/or point defects. Also, the exchange correlation functionals used in DFT calculations are not exact, and this approximation may lead to errors of similar order of magnitude as the difference in energy between the various ordered structures.[16–18] Additionally, only ordered structures can be simulated using DFT, since the calculations require a unit cell. Finally, a systematic exploration of all the possible adsorbate distributions within a unit cell would require many calculations, given the size of the unit cell and the three sites per surface atom available. In practice one therefore checks only a very limited number of adsorbate structures, accepting the risk that the actual ordered structure is overseen.[18,19] Only more recently do people combine statistical methods with large sets of calculations to get better estimates of lateral interactions.[20–23]

We have chosen to study this problem by means of a kinetic Monte Carlo lattice gas adsorption study. The use of Monte Carlo methods allows the efficient simulation of large numbers of adsorbates over an extended time. In a simulated adsorption experiment, the adsorbates are allowed to move around over the surface, and the system therefore finds by itself which ordered structure (if any) is most relevant as the coverage increases. The ordered structures found in this work are therefore an outcome of the model, they are not specified beforehand. As an input for the model we use some simple and straightforward rules on how the adsorbates interact with other adsorbates and with the surface. In addition to this we have checked whether small changes in the rules or values for the interactions affect the overall ordering behaviour. In the model we used the lattice gas approximation, *i.e.*, assumed that all adsorbates occupy either bridge or top sites. This is in agreement with the common understanding in literature, though some older studies have suggested off-lattice models for CO as well.

Lattice gas adsorption studies have mostly focussed on top (or equivalently fourfold) site adsorption.[24–26] Less studies have been devoted to bridge site adsorption.[27–29] The case for CO adsorption, with both top and bridge sites being occupied, has received even less attention. In some cases the CO adsorption has been simplified, by including either only bridge, or only top sites. This is a reasonable approximation for low coverages, and has been used by, amongst others, King and Jansen.[30–32] Zhdanov *et al*. used the full model with both top and bridge sites, and studied the relative occupation of top and bridge sites as a function of total coverage. The methodology used in that work did not allow the determination of ordered structures, however.[33,34] Liu *et al*. have studied the full system of top, bridge and fourfold site, but they focussed their effort on coverages below 0.50 ML CO.[35,36] Persson, on the other hand, conducted an extensive study of the adorption and ordering with combined top and bridge site adsorption, however this was for the fcc(111) surface, not for the fcc(100) surface.[24,37,38] It also needs to be mentioned that a lot of research has been done to construct complete phase diagrams for adlayer systems, amongst others by Binder *et al*.[25]

In this work we focus on the case of CO adsorption on the (100) surface of platinum and rhodium, where both top and bridge sites are occupied. We show how a simple lattice gas model, with a minimum number of parameters, is able to explain the adsorption and ordering behaviour of CO on these surfaces. We also suggest, based on this model, a refinement of the distribution of adsorbates within the unit cell of some of the ordered structures found for CO on the (100) surface of platinum and rhodium.

2. Model

We model the adsorption of a molecule M from the gas phase on the top and bridge sites of an fcc(100) surface by Monte Carlo simulations employing a lattice-gas model for the substrate:

$$\mathrm{M_{gas}} + * \leftrightarrows \mathrm{M_{ads,top}} \quad (1)$$

$$\mathrm{M_{gas}} + ** \leftrightarrows \mathrm{M_{ads,bridge}} \quad (2)$$

$$\mathrm{M_{ads,bridge}} \leftrightarrows \mathrm{M_{ads,top}} + * \quad (3)$$

where * denotes an empty site on top of a surface atom, and ** denotes an empty bridge site (formed by two empty surface atoms).

We consider a shell of purely hard interactions, in which the simultaneous bonding of two molecules to neighbouring sites is simply excluded. These excluded neighbouring sites around an occupied top or bridge site are indicated by an *X* in Table 1 for each model (A–G, and the models for CO on Pt(100) and Rh(100)). The exclusion of the first shells of neighbouring sites is a common approximation related to the fact that the metal–metal distance is usually smaller than the van der Waals diameter of the adsorbate.[26,27,39] Significant repulsion is therefore expected if two adsorbates bind this close together. In some cases we also consider a shell of finite interactions, these are indicated by φ_i in Table 1 and shown in Fig. 1.

One additional adsorbate–adsorbate interaction has been included in all models. It concerns the close adsorption of multiple bridge-bound adsorbates. This interaction is discussed in Fig. 2. In Fig. 2a two bridge-bound adsorbates are shown, where each adsorbate binds to different substrate atoms. If the adsorbates are moved closer to each other, we get the situation as depicted in Fig. 2b. Now, the adsorbates share one substrate atom. Since each surface atom has only a limited

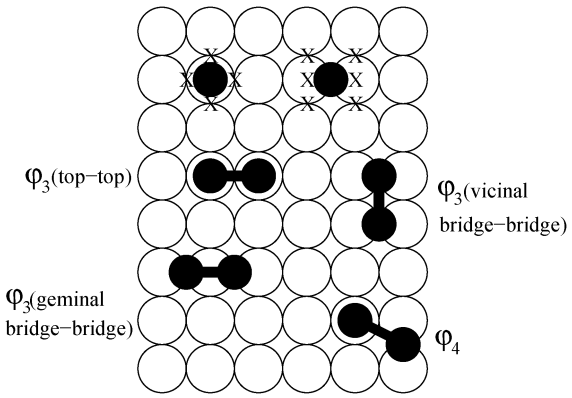

Fig. 1 Top part: excluded sites (indicated by an X) at $\frac{1}{2}$ and $\frac{1}{2}\sqrt{2}$ lattice vectors distance around a top and a bridge bound adsorbate. Middle and lower left part: the three different interactions at 1 lattice vector distance: the top–top interaction φ_3(t–t), the geminal bridge–bridge interaction φ_3(*gem* b–b) with both adsorbates binding to the same substrate atom, and the vicinal bridge–bridge interaction φ_3(*vic* b–b) with both adsorbates binding to neighbouring substrate atoms. Bottom right: the φ_4 interaction between a top and a bridge bound adsorbate at $\frac{1}{2}\sqrt{5}$ lattice vectors distance.

substrate atoms takes place, and therefore no bond weakening is expected. The only excluded configuration is therefore the one presented in Fig. 2c. The reason why the situation viewed in Fig. 2c is expected to be much worse than the one viewed in Fig. 2b, is the following. In Fig. 2b, each adsorbate still binds to one substrate atom that does *not* have bonds to other adsorbates. A weakening of the bond with the shared substrate atom may therefore be (partially) compensated by a strengthening of the bond with the non-shared substrate atom. This compensation is only possible in the situation presented in Fig. 2b, but not in the situation in Fig. 2c, since both substrate atoms are shared in the latter case.

In most simulations, the difference in adsorption energy between top and bridge sites has been set to zero (by taking the adsorption and desorption rate constants equal for both types of sites). Only for the case of model F and the models for CO on Pt(100) and CO on Rh(100) has an adsorption energy difference between the top and bridge sites been taken into account.

The adsorption isotherms were calculated by including adsorption, desorption and surface diffusion steps and varying the simulated gas phase pressure P_M. The simulations were

Table 1 Lateral interactions employed in the different models. An *X* indicates that no other adsorbate may bind on a site which is separated from an adsorbate by the specified distance. This is equivalent to stating that there is an infinitely repulsive interaction between two adsorbates separated by the indicated distance. A φ indicates that there is a finite interaction between two adsorbates separated by the indicated distance. A positive value for the interaction indicates a repulsion between the adsorbates. The values between brackets indicate the size of the interactions in kJ mol^{-1} at a simulated adsorption temperature of 150 K

	Distance between sites (lattice vectors)			
	1	1	1	$\frac{1}{2}\sqrt{5}$
Model distance between sites interaction	φ_3(*vic* b–b)	φ_3(*gem* b–b)	φ_3(t–t)	φ_4
A				
B	*X*	*X*	*X*	
C	*X*	*X*	*X*	*X*
D	φ_3(*vic* b–b) = φ_3(*gem* b–b) = φ_3(t–t), $4k_BT/6k_BT/8k_BT$			
E	*X*	*X*	*X*	$2k_BT/4k_BT/6k_BT$
F	*X*	*X*	*X*	
	+ top/bridge adsorption energy difference of $2k_BT/4k_BT/6k_BT/8k_BT$			
G	$4k_BT/6k_BT$	$4k_BT/6k_BT$	$4k_BT/6k_BT$	
CO/Pt(100)	$4k_BT$–$8k_BT$	$8k_BT$	$8k_BT$	
	(5.0–10.0)	(10.0)	(10.0)	
	+ top/bridge adsorption energy difference of $4k_BT$ (5.0)			
CO/Rh(100)	$3.5k_BT$	$2.7k_BT$	$10.7k_BT$	$3.3k_BT$
	(4.4)	(3.3)	(13.3)	(4.2)
	+ top/bridge adsorption energy difference of $5.2k_BT$ (6.5)			

bonding capacity, the adsorbate–substrate bond indicated in grey will be somewhat less strong. The total binding energy for the situation depicted in Fig. 2b will therefore be less than for the situation in Fig. 2a. Adding one more adsorbate to the situation in Fig. 2b will bring up the situation depicted in Fig. 2c. The center adsorbate in this case binds to two substrate atoms which also have bonds to other adsorbates. This strongly reduces the binding strength of the center adsorbate, and this situation is therefore excluded from our simulations. Adding other adsorbates in top sites to the situation depicted under Fig. 2b results in Fig. 2d. In this case there is no additional sharing of substrate atoms, so no additional bond weakening is expected. Finally, for the case of top-bound adsorbates only, Fig. 2e, no sharing of the

performed with the program CARLOS†.[40,41] Increasing the simulated gas phase pressure of the molecule M causes a shift in the adsorption–desorption equilibrium and thus an increase in the surface coverage of the adsorbed molecule M. The ratio of the adsorption to desorption rate constant k_{ads}/k_{des} equals

$$k_{ads}/k_{des} = KP_M, \quad (4)$$

with P_M as the gas phase pressure of molecule M, and *K* *a constant*.

† CARLOS is a general-purpose program, written in C, for simulating reactions on surfaces that can be represented by regular grids; an implementation of the first-reaction method and the variable stepsize method, written by J. J. Lukkien.

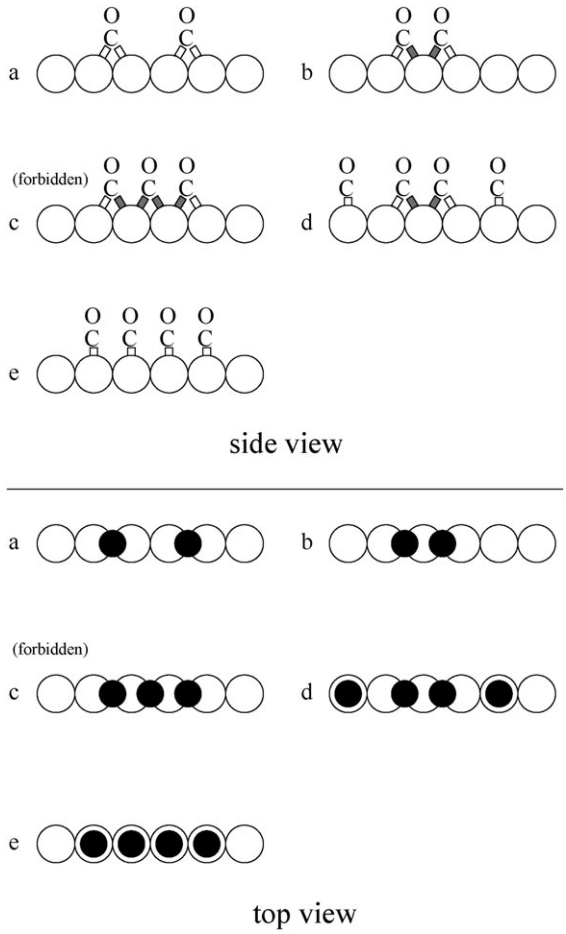

Fig. 2 Lateral interaction model involving multiple adsorbates bonding in a bridged fashion: (a) two bridge-bound adsorbates far apart each, bond to different surface atoms, (b) two bridge-bound adsorbates close together share a single surface atom; the bonds to this atom (in grey) are less strong than the bonds to the other surface atoms, (c) with three bridge-bound adsorbates close together, the middle adsorbate bonds only to surface atoms which also bond to other adsorbates; this situation is forbidden in our simulations, (d) with two bridge-bound adsorbates close together and additional top-bound adsorbates, each bridge-bound adsorbate binds to one non-shared surface atom, and (e) with only top-bound adsorbates close together, no surface atoms are shared between the adsorbates. The upper panel shows a side view for extra clarity, the lower panel shows a top view, used in the remainder of the article.

The algorithm used was the first reaction method. In this algorithm, a tentative time is calculated for every possible reaction. All reactions together with their tentative times are stored in an event list. The algorithm proceeds by repeatedly performing the following steps: select the reaction with minimal time from the event list, advance the system time to the time of this reaction, adjust the lattice according to the reaction, and update the event list. For the case of time-dependent rate constants (such as in these simulations, where adsorption and desorption rate constants are time dependent because the gas phase pressure changes with time), one can determine exactly the tentative times or approximate them by taking the rate constants constant for a small time step. In this work the times were determined exactly. Using kinetic Monte Carlo simulations rather than equilibrium Monte Carlo
simulations allowed us to study also the non-equilibrium adsorption of adsorbates, which is important for high adsorption rates (*i.e.*, high gas phase pressures).

The diffusion steps were defined as hopping from a top site to a neighbouring bridge site or *vice versa*. Both the adsorption/desorption couple and the diffusion reactions were defined to satisfy detailed balance. This means that in all cases the effect of the difference in binding energy between top and bridge sites, and the effect of the lateral interactions have been accounted for by multiplying the base rate constants with an appropriate factor.

The simulated adsorption isotherm was determined by increasing the simulated pressure of M as a function of time, thus shifting the adsorption equilibrium. This pressure increases exponentially according to

$$P_{\mathrm{M}} = P_{\mathrm{M},0}\exp\beta t \tag{5}$$

with $P_{\mathrm{M},0}$ the initial pressure of M, t equals time, and β a constant which determines the rate at which the pressure increases. The base rate constants for adsorption and desorption were defined as

$$k_{\mathrm{ads}} = k_0 P_{\mathrm{M}}^{\frac{1}{2}} \tag{6}$$

$$k_{\mathrm{des}} = k_0 P_{\mathrm{M}}^{-\frac{1}{2}}, \tag{7}$$

where k_0 is a constant. The main argument for using this definition of adsorption (instead of regular constant pressure adsorption) is that in this way adsorption equilibrium can be easily established for a large range of $k_{\mathrm{ads}}/k_{\mathrm{des}}$. The actual rate constants for adsorption, desorption and diffusion were determined from the base rate constants (k_{ads},k_{des} and the base rate constant for diffusion $k_{\mathrm{diff},0}$) by multiplying them with a factor f to account for the effect of the lateral interactions and the difference in binding energy between top and bridge sites:

$$k'_{\mathrm{ads}} = f' k_{\mathrm{ads}} \tag{8}$$

$$k''_{\mathrm{des}} = f'' k_{\mathrm{des}} \tag{9}$$

$$k'''_{\mathrm{diff}} = f'' k_{\mathrm{diff},0} \tag{10}$$

This type of definition is fully equivalent to the one used in a previous study of anion adsorption under electrochemical conditions.[27]

The factors k_0, $k_{\mathrm{diff},0}$, and β determine the adsorption and equilibration behaviour. Good equilibration was typically found for $k_0 = 10^3\ \mathrm{s}^{-1}$, $k_{\mathrm{diff},0} = 10^5\ \mathrm{s}^{-1}$ and $\beta = 10^{-1}\mathrm{s}^{-1}$. Equilibration was checked by looking for hysteresis between simulated adsorption and desorption isotherms, and by comparing adsorption isotherms calculated with different values of k_0, $k_{\mathrm{diff},0}$, and β. The temperature in the simulations was fixed at 150 K. All snapshots represent only a small part of the simulated grid, the full simulated grid consisted of 120×120 sites. Due to the large size of the ordered domains, usually only one domain orientation is shown in the figures, but we wish to emphasise that all possible domain orientations are found when looking on the scale of the full simulated grid.

3. Results

3.1 The hard sphere models A–C

We first study the behaviour of the hard-sphere models A, B, and C. For model A, the sites at $\frac{1}{2}$ and $\frac{1}{2}\sqrt{2}$ distance are excluded (see the overview in Tables 1 and 2). At low coverages (less than 0.01 ML), one-third of the adsorbates resides in top sites, while two-thirds of the adsorbates reside in bridge sites. This reflects the relative abundance of top and bridge sites on the surface: one top site for every two bridge sites. Since the adsorbates are modelled to bind equally strongly to both types of sites, the relative occupation is therefore one-third *versus* two thirds.

For total coverages below 0.5 ML, the coverage of bridge-bound adsorbates remains higher than the coverage of top-bound adsorbates. At a total coverage of about 0.5 ML, the ratio has lowered to one, *i.e.*, for every top-bound adsorbate there is one bridge-bound adsorbate. For a total coverage larger than 0.5 ML, the top-bound adsorbates dominate. The saturation coverage for this model is 1.00 ML, and a p(1 × 1) structure is formed with all adsorbates bound in top sites (see Fig. 3, top left structure and the overview in Table 2).

The fact that at low coverage the majority of the adsorbates are bound to bridge sites, while at high coverage almost all adsorbates are bound to top sites, can be rationalised as follows. At low coverage, as mentioned above, the relative amount of available sites is determining, while at high coverage the interactions between the adsorbates are determining. The restriction in Fig. 2c limits the total coverage for a bridge-bound-only system to 0.67 ML. The bridge site is therefore shunned at high coverage, and the top site, which has no such restriction, is used instead.

For model B, the sites $\frac{1}{2}$, $\frac{1}{2}\sqrt{2}$, and 1 distance are excluded. At low coverage, once again one-third of the adsorbates resides in top sites, while two-thirds of the adsorbates reside in bridge sites. At saturation, the bridge and top occupancies are equal, while at all coverages below saturation point more adsorbates are bound to bridge sites than to top sites. The saturation coverage is two-thirds of a monolayer, with half of the adsorbates bound to top sites, half of the adsorbates bound to bridge sites.

At saturation, the adlayer turns out to be one-dimensionally ordered. Adsorbates occupy alternatingly a top and a bridge site, as indicated by the arrows in the upper part of Fig. 4. Now, for each top-bound adsorbate at the top of the figure, the nearest neighbour top-bound adsorbate can be located at the lower left, or at the lower right side of the original adsorbate. Local patches of two-dimensionally ordered structures form, depending on where this next top-bound adsorbate is found. The relation between top-bound adsorbates in

Table 2 Ordered adlayer structures found for the different models

	Coverage/ML				
Model	0.50	0.67	0.75	0.83	1.00
A	—	—	—	—	p(1 × 1)–1t
B	—	one-dim. and $(3\sqrt{2} \times \sqrt{2}) - 2t + 2b$			
C	c(2×2)–2b $(2\sqrt{2} \times \sqrt{2}) - 2b$				
D	—	one-dim. and $(3\sqrt{2} \times \sqrt{2}) - 2t + 2b$	—	c(6 × 2)–6t + 4b	p(1 × 1)–1t
E	c(2 × 2)–2b $(2\sqrt{2} \times \sqrt{2}) - 2b$	one-dim. and $(3\sqrt{2} \times \sqrt{2}) - 2t + 2b$			
F	c(2×2)–2t	one-dim. and $(3\sqrt{2} \times \sqrt{2}) - 2t + 2b$	—		
G	—	—	c(4 × 2)–4t + 2b or c(4 × 2)–2t + 4b	c(6 × 2)–6t + 4b	p(1 × 1)–1t
CO/Pt(100)	c(2 × 2)–2t	one-dim. and $(3\sqrt{2} \times \sqrt{2}) - 2t + 2b$	c(4 × 2)–4t + 2b	c(6 × 2)–6t + 4b	p(1 × 1)–1t
CO/Rh(100)	c(2 × 2)–2t	—	$(2\sqrt{2} \times \sqrt{2}) - t + 2b$ + (4 × 2)–2t + 4b	c(6 × 2)–6t + 4b	p(1 × 1)–1t

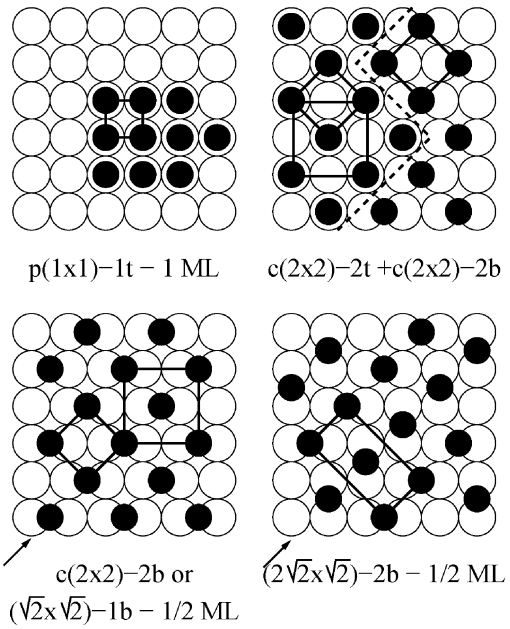

Fig. 3 Ordered structures found for the hard sphere models A (top left) and C (bottom). Model A yields a p(1 × 1) structure. For model C, one-dimensional ordering along the direction of the arrows is found. Local patches will order into, respectively, a c(2 × 2) and a $c(2\sqrt{2} \times \sqrt{2})$ structure. Top right: c(2 × 2)−2t and c(2 × 2)−2b islands as found in model E for coverages larger than 0.50 ML.

subsequent rows is indicated by the dotted line. In one case, the local adsorbate structure resembles a (3 × 2) unit cell, in another a (4 × 3) unit cell. If the top-bound adsorbates in subsequent rows line up consistently, a $(3\sqrt{2} \times \sqrt{2})$ structure is formed. The chance that a top-bound adsorbate in the next row is at the lower left side, is equal to the chance that a top-bound adsorbate in the next row is at the lower right side: one-half. The relative size and abundance of these patches is purely determined by statistics. This means that in general only a small part of the adlayer will be found to correspond to the experimentally observed $(3\sqrt{2} \times \sqrt{2})$ unit cell.

For model C, all sites up to a distance of $\frac{1}{2}\sqrt{5}$ are excluded. At low coverage, one-third of the adsorbates resides in top sites, while two-thirds of the adsorbates reside in bridge sites. At saturation, only bridge-bound adsorbates are present. At all intermediate coverages more adsorbates are bound to bridge sites than to top sites. The saturation coverage is 0.50 ML, and a one-dimensional ordering is found along the direction of the arrow (Fig. 3, bottom part). This type of one-dimensional ordering is identical to the one found for the case of bridge-site only adsorption.[27–29] Local patches will order into, respectively, a $(2\sqrt{2} \times \sqrt{2})$ and a c(2 × 2) structure, as indicated at the bottom part of Fig. 3. A c(2 × 2)–2t structure with all adsorbates in top sites (see Fig. 3, top right) was not found in these simulations. Such a structure is equal in energy to the $(2\sqrt{2} \times \sqrt{2})$ and a c(2 × 2) structures with all adsorbates in bridge sites, since there is no energy difference between top and bridge sites in this model. However, the structure with only the bridge sites is only one-dimensionally ordered, giving it an entropic advantage over the two-dimensionally ordered pure c(2 × 2) structure with all adsorbates in top sites.

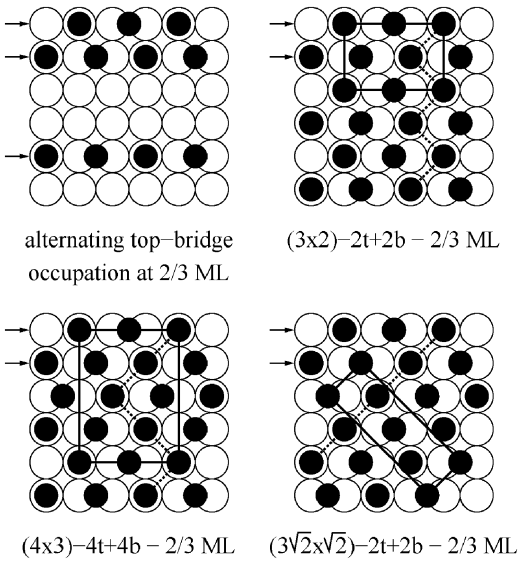

Fig. 4 Adsorbate configurations found at saturation for the hard sphere model B. At a coverage of 0.67 ML, the adsorbates alternatingly occupy top and bridge sites (top left). The ordering is therefore essentially one-dimensional. Depending on the placement of each subsequent row of adsorbates, patches of a (3 × 2) (top right), a (4 × 3) (bottom left), and the experimentally observed $(3\sqrt{2} \times \sqrt{2})$ ordered structure (bottom right) are found.

3.2 Models with finite interactions D–G

For each of the hard sphere models discussed above, ordered structures are only found at one coverage. In the experiments for CO adsorption, however, several subsequent ordered structures are found at coverages between 0.50 and 0.83 ML. This can be explained by the presence of finite lateral interactions in addition to the hard-sphere interactions as modelled in the models A, B, and C. The models D to G are used to investigate the influence of finite interactions (in addition to hard-sphere interactions) on the ordering behaviour of the adsorbate.

3.2.1 Models with one finite interaction. Model D assumes exclusion of sites at a distance of $\frac{1}{2}$ and $\frac{1}{2}\sqrt{2}$, with a finite interaction φ_3 for adsorbates at 1 distance. The finite interaction was set to either $4k_BT$, $6k_BT$ or $8k_BT$ (equivalent to 10, 15 or 20 kJ mol^{-1} at 300 K). Based on the results for models A and B, one expects two ordered structures for model D: the p(1 × 1) ordered structure at 1.00 ML, with only top-bound adsorbates, and the one-dimensionally ordered structure at 0.67 ML with half the adsorbates in top sites, the other half in bridge sites. The ordering into top-bridge lines at 0.67 ML is observed for interaction φ_3 equal to $6k_B$T or $8k_B$T, not for φ_3 equal to $4k_B$T. Apparently, an interaction of $4k_B$T is not sufficient to force the adsorbates into the one-dimensionally ordered structure. Up to about 0.67 ML, more adsorbates bind to bridge sites than to top sites; above 0.67, the reverse is true. At saturation the p(1 × 1) ordered structure with all adsorbates in top sites is found irrespective of the value of the interaction φ_3. Several new structures are also found, in addition to these structures, at coverages between 0.80 and 0.85 ML. These additional structures are shown in Fig. 5.

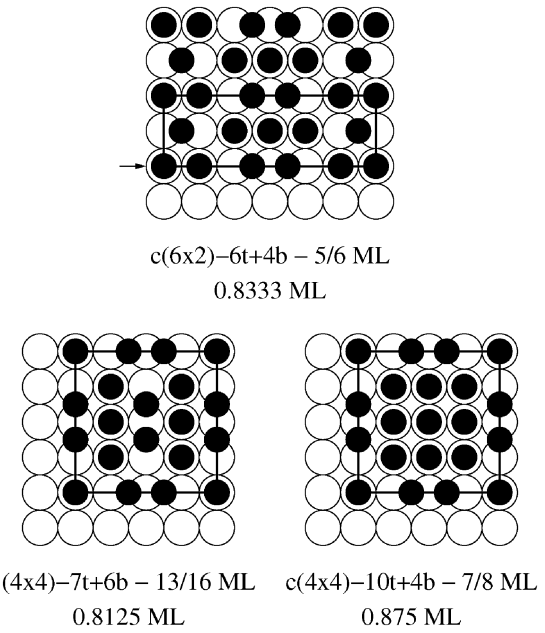

Fig. 5 Additional ordered structures found for the finite interaction model D.

The main ordered structure found in the 0.80 to 0.85 ML coverage region is the c(6 × 2) ordered structure (top). This structure is found for all studied values of the interaction φ_3. The unit cell of this ordered structure contains 6 top bound and 4 bridge bound adsorbates, resulting in a total coverage of $\frac{5}{6}$ or 0.83 ML. Typical of this ordered structure is that the adsorbates occupy alternatingly three times a top site, and next two times a bridge site (see the arrow). At coverages just below 0.83 ML, the c(6 × 2) ordered structure is found together with patches of the (4 × 4) structure (bottom left, with a coverage of $\frac{13}{16}$ ML). At coverages above 0.83 ML, a combination of patches of the c(6 × 2) ordered structure with patches of the c(4 × 4) structure (bottom right, with a coverage of $\frac{7}{8}$ ML) is found.

Model E assumes exclusion of sites at a distance of $\frac{1}{2}$, $\frac{1}{2}\sqrt{2}$ and 1, with a finite interaction φ_4 for adsorbates at $\frac{1}{2}\sqrt{5}$ distance. The finite interaction was set to either $2k_B$T, $4k_B$T or $6k_B$T (equivalent to 5, 10 or 15 kJ mol^{-1} at 300 K). Based on the results for model B and C, one expects two ordered structures for model E: the one-dimensionally ordered structure at 0.67 ML with half the adsorbates in top sites, the other half in bridge sites, and the one-dimensionally ordered structure at 0.50 ML with all adsorbates in bridge sites. The saturation ordering into top-bridge lines at 0.67 ML is observed for all values of the interaction φ_4, with patches of the $(3\sqrt{2} \times \sqrt{2})$ structure present. The one-dimensional ordering at 0.50 ML (with patches of the c(2 × 2) and the $(2\sqrt{2} \times \sqrt{2})$ structure) is only observed for φ_4 larger or equal to $3k_B$T.

A striking adlayer transformation takes place at a coverage just above 0.50 ML (see Fig. 3, top right). The one-dimensionally ordered structure disappears fully, and instead c(2 × 2)–2t islands with all adsorbates in top sites, and c(2 × 2)–2b islands with all adsorbates in bridge sites are formed. These different islands are separated by "dense" domain walls (dashed line), thus allowing a coverage slightly higher than 0.50 ML. No $(2\sqrt{2} \times \sqrt{2})$ structure is found above 0.50 ML coverage.

No additional structures are found for the finite interaction model E. For coverages between 0.00 and 0.50 ML both top and bridge bound adsorbates are present, but bridge bound adsorbates are more abundant. At exactly 0.50 ML, only bridge bound adsorbates are present. At coverages between 0.50 and 0.67 once again both top and bridge bound adsorbates are present. At saturation (0.67 ML), equal amounts of bridge and top bound adsorbates are present.

3.2.2 Differentiation in the adsorption energy of top and bridge sites. Model F assumes exclusion of sites at a distance of $\frac{1}{2}$, $\frac{1}{2}\sqrt{2}$ and 1, with a difference in binding energy between the top and the bridge sites. The difference in binding energy between the top and bridge sites was varied from $0k_B$T (Model B), to $2k_BT$, $4k_BT$, $6k_BT$, and $8k_BT$. In all except the first case the adsorbate binds more strongly to the top site than to the bridge site. The results for the $0k_BT$ energy difference is by definition identical to the case of Model B. The results for an energy difference of $2k_BT$ and upwards are comparable to the ones for Model B: the same ordered structures at the saturation coverage of 0.67 ML, but at intermediate coverages an increasing preference for binding to the top sites is shown. This becomes very apparent at a difference of $4k_BT$ and above, where at 0.50 ML coverage a new c(2 × 2)–2t ordered structure is formed with all adsorbates in top sites. This is purely due to the difference in adsorption energy of top sites on the one hand and bridge sites on the other hand.

3.2.3. Differentiation in the φ_3 interaction. Model G, just like model D, has a finite interaction at 1 distance. As shown in Fig. 1, there are actually three different interactions at this distance: the interaction between two neighbouring top bound adsorbates (φ_3(t–t)), the interaction between two bridge bound adsorbates that share a surface atom (φ_3(*gem* b–b)), and the interaction between two bridge bound atoms that do not share a surface atom (φ_3(*vic* b–b)). For model D we assumed for the value of all these three interactions to be identical. However, there is no *a priori* reason why this should be true, so we also investigate the case where the various φ_3 interactions differ. Each φ_3 interaction was set to either $4k_BT$ or $6k_BT$ (10 or 15 kJ mol^{-1} at 300 K), and the results of the 8 simulations are summarised below. For all combinations, at 0.83 ML the c(6 × 2) ordered structure and at 1.00 ML the p(1 × 1) ordered structure are found. The one-dimensional ordering and $(3\sqrt{2} \times \sqrt{2})$ ordered structure at 0.67 ML are, similar to model D, not found when one of the interactions equals $4k_BT$.

However, a significant difference arises at 0.75 ML. For all three φ_3 equal in value, no ordered structure is found at this coverage. If φ_3(*gem* b–b) > φ_3(t–t), then a c(4 × 2)–4t + 2b structure as depicted in the left part of Fig. 6 is found. In this structure, the majority of the adsorbates bind to top sites. The adsorbates form lines of top–top-bridge, as indicated by the arrow. This structure is only stable in a very small region, it converts rapidly into a p(1 × 1) ordered structure. If, on the other hand, φ_3(*gem* b–b) < φ_3(t–t), then a different c(4 × 2) structure as depicted in the right part of Fig. 6 is found. In this c(4 × 2)–2t + 4b structure, the majority of the adsorbates

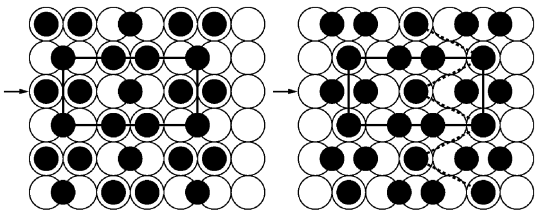

Fig. 6 Additional ordered structures found for the finite interaction model G, when the φ_3 interaction is differentiated as described in Fig. 1. If $\varphi_3(gem$ b–b) > φ_3(t–t), then the c(4 × 2) structure on the left is formed. If $\varphi_3(gem$ b–b) < φ_3(t–t), then the c(4 × 2) structure on the right is formed.

bind to bridge sites. The adsorbates form lines of bridge–bridge-top, as indicated by the arrow. This second c(4 × 2) structure is stable over a large region, it does not convert as fast into a p(1 × 1) structure as the first one.

It is obvious why this interchange in structures takes place: if the repulsion between two neighbouring top bound adsorbates is smaller than between two neighbouring bridge bound adsorbates, the structure on the left is more stable than the one on the right, and *vice versa*. One can even think of this as a one-dimensional compression of the adlayer (in the direction of the arrow) as the coverage increases, and depending on the strength of the individual interactions, either one structure will be formed, or the other. No ordered structure is found for $\varphi_3(gem$ b–b) = φ_3(t–t), since then there is no driving force that will make the system prefer one ordered structure over the other. Please note that $\varphi_3(vic$ b–b) has no influence on this interchange, since it is found in neither of the two ordered structures.

3.3 Model for CO on Pt(100)

The model for CO on Pt(100) assumes exclusion of sites at a distance of $\frac{1}{2}$ and $\frac{1}{2}\sqrt{2}$, has a finite repulsive interaction of $8k_BT$ at distance 1, and also includes a difference of $4k_BT$ in binding energy between the top and the bridge site. The reasoning behind this choice of parameters is listed in section 4.

For coverages below 0.50 ML, the majority of the CO molecules bind to top sites. At 0.50 ML, a c(2 × 2)–2t ordered structure is found with most of the adsorbates (0.45 ML or more) in top sites, and only a small amount of adsorbates (0.05 ML or less) in bridge sites. The bridge-bound adsorbates are defects in the otherwise ordered adlayer structure. The c(2 × 2)−2t structure is shown in Fig. 3, top right.

At 0.67 ML coverage, similar to model B, a second ordered adlayer is found. This is shown in Fig. 4: one-dimensional ordering with alternating top and bridge site occupation resulting in a $(3\sqrt{2} \times \sqrt{2})$ structure in parts of the adlayer. The third ordered structure is found at 0.75 ML coverage. This is the c(4 × 2)−4t + 2b structure displayed on the left-hand side of Fig. 6. This particular c(4 × 2) structure is more stable than the other one shown on the right side, since in this structure more adsorbates bind to the top sites, which have a higher adsorption energy than the bridge sites.

Finally, upon continued adsorption, a c(6 × 2) ordered structure is found at 0.83 ML coverage, identical to the one found for model D, and shown in Fig. 5. The distribution of the adsorbates over top and bridge sites varies strongly with coverage. This is shown in Fig. 7, top panel.

3.4 Model for CO on Rh(100)

The model for CO on Rh(100) assumes exclusion of sites at a distance of $\frac{1}{2}$ and $\frac{1}{2}\sqrt{2}$, has a finite repulsive interaction at 1 and $\frac{1}{2}\sqrt{5}$ distance, and also includes a difference in the binding energy between the top and the bridge site (for the values, see Table 1). The reasoning behind this choice of parameters is listed in section 4.

For coverages below 0.50 ML, the majority of the CO molecules bind to top sites. At 0.50 ML, a c(2 × 2)−2t ordered structure is found with most of the adsorbates (0.45 ML or more) in top sites, and only a small amount of adsorbates (0.05 ML or less) in bridge sites. The bridge-bound adsorbates are defects in the otherwise ordered adlayer structure. The c(2 × 2)−2t structure is shown in Fig. 3, top right.

At 0.67 ML coverage, contrary to the case of CO on Pt(100), no $(3\sqrt{2} \times \sqrt{2})$ structure is found. Only local ordering into top-bridge rows is seen. At 0.75 ML coverage a one-dimensionally ordered adlayer is found, with adsorbates forming top-bridge–bridge rows. This is shown in Fig. 8. Depending on how subsequent rows are placed with respect to neighbouring rows, locally a (4 × 2), a $(2\sqrt{2} \times \sqrt{2})$ and to a

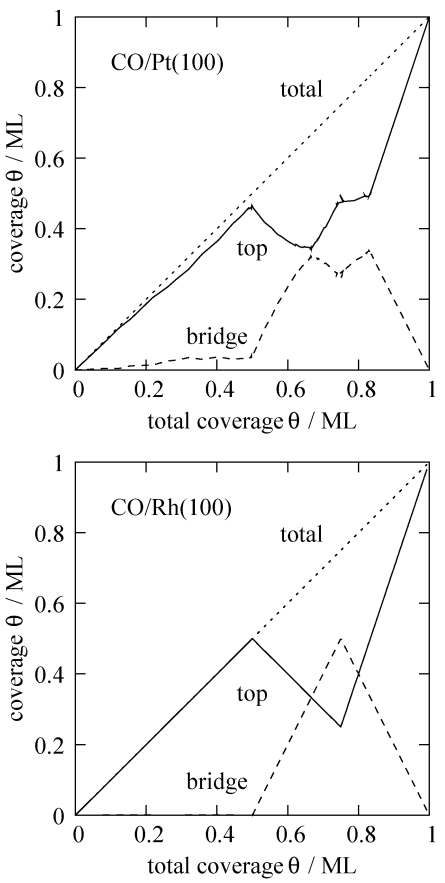

Fig. 7 Bridge and top site occupation as a function of coverage for the model of CO on Pt(100) (top), and the model of CO on Rh(100) (bottom).

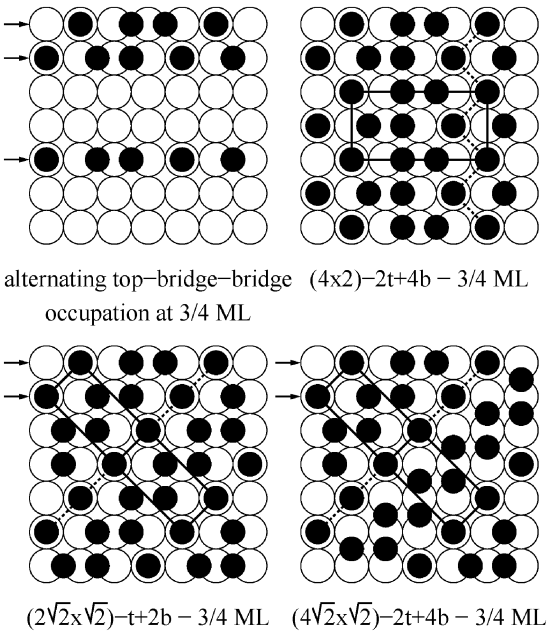

Fig. 8 Ordered structures found at 0.75 ML coverage for the model of CO on Rh(100).

lesser extent a $(4\sqrt{2} \times \sqrt{2})$ ordered structure are found. This case of one-dimensional ordering is analogous to the case of the one-dimensional ordering at 0.67 ML coverage found for Model B.

Finally, upon continued adsorption, a c(6 × 2) ordered structure is found at 0.83 ML coverage, identical to the one found for model D, and shown in Fig. 5. The distribution of the adsorbates over top and bridge sites varies strongly with coverage. This is shown in Fig. 7, bottom panel.

3.5 A simplified model

The exclusion, as described in Fig. 2, has an effect on which ordered structures are found. For completeness, we here also list the ordered structures found for models A to E when this exclusion of three bridge bound adsorbates next to each other is left out of the model. For model A, the saturation coverage remains 1.00 ML. Instead of a two-dimensionally ordered p(1 × 1) structure, a one-dimensionally ordered structure is found, consisting of rows of bridge bound adsorbates, mixed with rows with top bound adsorbates (thus forming a p(2 × 1)−t + b structure). For models B and C, no difference is seen in the ordered structures. In model D, the one dimensionally ordered structure at 0.67 ML is reproduced. The structure at 1.00 ML is no more a p(1 × 1), but one-dimensionally ordered with lines of bridge bound adsorbates and lines of top bound adsorbates. The c(6 × 2) structure is not found. For model E, no difference is seen in the ordered structures.

For the model of CO on Pt(100), the c(2 × 2)−2t, the one-dimensionally ordered structures at 0.67 ML, and the c(4 × 2)−4t + 2b structure are found. The c(6 × 2) structure is not found, and the saturation structure is a one-dimensionally ordered structure, consisting of rows of bridge bound adsorbates, mixed with rows with top bound adsorbates (thus forming a p(2 × 1)−t + b structure). For the model of CO on Rh(100), the c(2 × 2)−2t ordered structure is found at 0.50 ML, and at 1.00 ML the surface is fully occupied by bridge bound adsorbates in a p(1 × 1) structure. In-between, no ordered structures are found.

4. Comparison to experiment

4.1 CO on Pt(100)

Fig. 9 summarises the ordered structures as they have been reported for CO on Pt(100). A clear c(2 × 2) structure is observed experimentally at around 0.50 ML, which is mostly assigned to top-bound CO, but also sometimes to bridge bound CO. Vibrational spectroscopy, similar to Rh(100), indicates that both top and bridge bound adsorbates are present over the entire coverage range, with a clear preference for top occupation up to 0.50 ML, and a minimum in the bridge occupation at around 0.50 ML. At higher coverages a $c(5\sqrt{2} \times \sqrt{2})$ ordered structure, a $(3\sqrt{2} \times \sqrt{2})$ ordered structure, and a c(4 × 2) ordered structure at 0.75 ML coverage are found. Recently, under electrochemical conditions an even higher coverage could be attained, this resulted in a c(6 × 2) ordered structure at 0.83 ML coverage.[15] It is interesting to note that experimentally both the c(4 × 2)−4t + 2b and c(4 × 2)−2t + 4b structures have been suggested. The STM study by Wakisaka favours the c(4 × 2)−4t + 2b model. It also needs to be mentioned that at low CO coverages the Pt(100) surface can show reconstruction. This reconstruction, however, is lifted above 0.05 ML coverage, and is therefore not relevant to the simulation of the high coverage ordered structures in this work.[42]

From these observations one can construct the parameters of our model. First, based on the low coverage preference of CO to bind to top sites, it is clear that there must be an adsorption energy difference between the top and bridge sites, in favour of the top site. Model F indicated that an energy difference of at least $4k_BT$ was necessary to produce a c(2 × 2)−2t structure at 0.50 ML (in the absence of other interactions). The value of $4k_BT$ therefore serves as a good starting point. Model D indicated that by taking a sufficiently large φ_3, one can produce both the $(3\sqrt{2} \times \sqrt{2})$ and the c(6 × 2) ordered structures. A series of simulations with increasing φ_3 indicated that a minimum value of $\varphi_3 = 8k_BT$ was needed to produce the $(3\sqrt{2} \times \sqrt{2})$ and the c(6 × 2) ordered structures with the previously determined difference between top and bridge adsorption energy. Finally, it was concluded that in Model D no ordered structure formed at 0.75 ML, since the c(4 × 2)−4t + 2b and c(4 × 2)−2t + 4b structures are equal in energy. In this model for the CO on Pt(100) case, however, there is a clear preference for the top site (of $4k_BT$), thus a c(4 × 2)−4t + 2b ordered structure is observed at 0.75 ML, in full agreement with the STM study of Wakisaka *et al.*[15] The only experimentally reported structure that was not reproduced in our model is the $c(5\sqrt{2} \times \sqrt{2})$ ordered structure at 0.60 ML.

It is important to note that the values listed in Table 1 for the interactions on Pt(100) are lower limits. The four ordered structures are found for a wide range of values. It is not

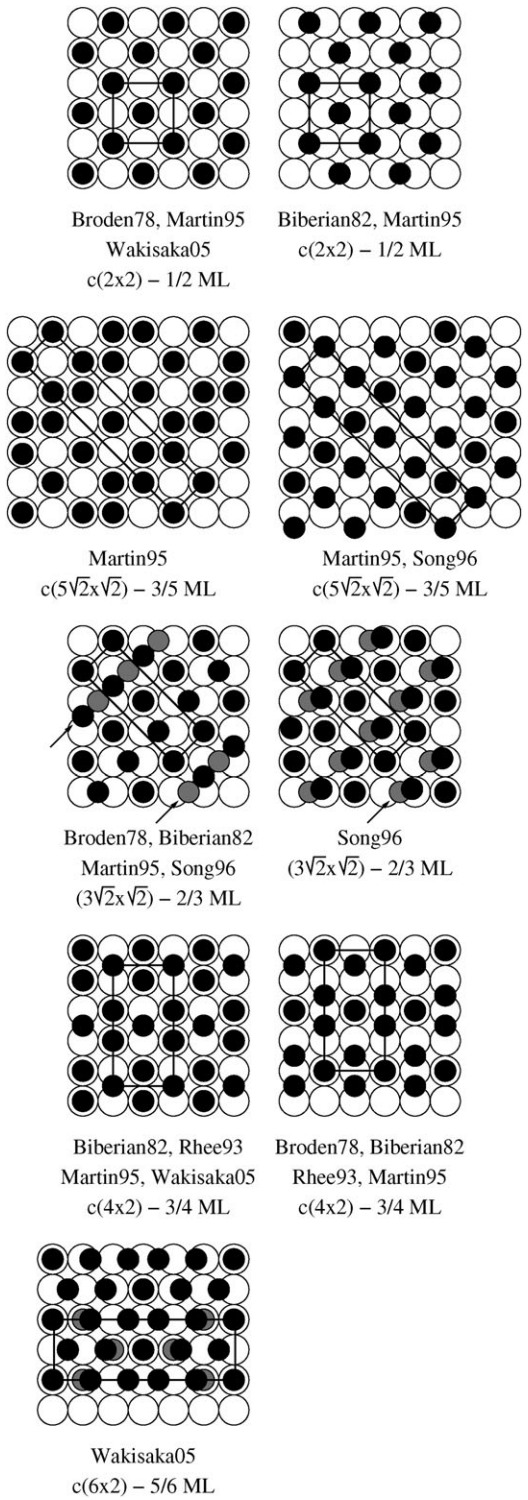

Fig. 9 Experimentally reported ordered structures for CO on the Pt(100) surface.[8,11,15,42–45] The black circles indicate the positions of the CO molecules as reported in the literature, grey circles indicate the alternative positions of the CO molecules according to the outcome of our model.

possible to establish the exact value of each interaction parameter by only looking at the ordered structures at one temperature value. For the sake of completeness the different φ_3 parameters were also varied individually. In this parameter search it turned out that the φ_3(*vic* b–b) interaction can be less repulsive than the other two φ_3 interactions.

4.2 CO on Rh(100)

Fig. 10 summarises the ordered structures as they have been reported for CO on Rh(100). A clear c(2 × 2) structure is observed experimentally at around 0.50 ML, which is mostly assigned to top-bound CO. Vibrational spectroscopy, similar to Pt(100), indicates that both top and bridge bound adsorbates are present over the entire coverage region, with a clear preference for top occupation up to 0.50 ML, and a minimum in the bridge occupation at around 0.50 ML. At a

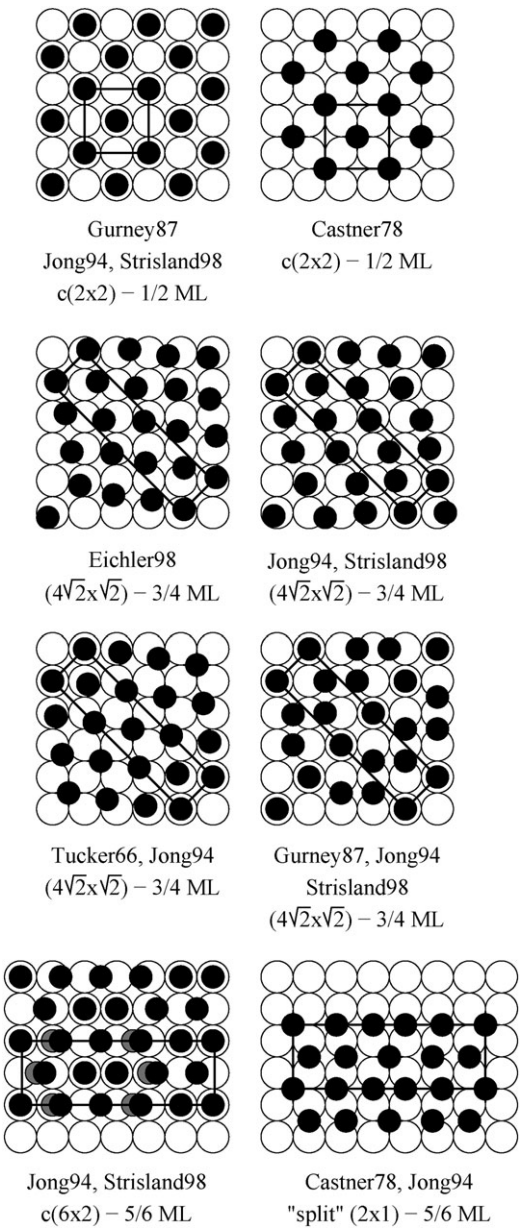

Fig. 10 Experimentally reported ordered structures for CO on the Rh(100) surface.[5,7,10,12,18,46,47] The black circles indicate the positions of the CO molecules as reported in the literature, the grey circles indicate the alternative positions of the CO molecules according to the outcome of our model.

higher coverage of 0.75 ML a $(4\sqrt{2} \times \sqrt{2})$ ordered structure is found, this coverage is also the high temperature (300 K) saturation coverage. Adsorption at lower temperatures (150 K) leads to an additional c(6 × 2) ordered structure, at 0.83 ML saturation coverage. It is interesting to remark that the energy difference between top and bridge bound CO is so small that background hydrogen adsorption can cause the CO to shift from one type of site to the other.[48–50] This can explain for a large part the differences in IR intensities for top and bridge bound CO reported by different authors.

The case for CO on Rh(100) shows a striking similarity to the case of CO on Pt(100): both have a c(2 × 2) structure at 0.50 ML coverage, an ordered structure at 0.75 ML coverage, and a c(6 × 2) saturation structure. The difference lies in the absence of a structure at 0.67 ML coverage for CO on Rh(100), and a $(4\sqrt{2} \times \sqrt{2})$ instead of a c(4 × 2) ordered structure at 0.75 ML coverage. In view of the similarity, the parameters used for the CO on Pt(100) model can serve as a good starting point to search for the parameters applicable to CO on Rh(100).

Based on the difference in ordered structures and the shape of the experimental TPD, appropriate parameters can be found, which mimick the ordering behaviour of CO on Rh(100); the c(2 × 2) ordered structure, a structure similar to the $(4\sqrt{2} \times \sqrt{2})$ structure and the c(6 × 2) ordered structure, as well as the distribution of CO over top and bridge sites as a function of coverage (Fig. 7, bottom panel). These values are listed in Table 1. In a subsequent publication we discuss in more detail this parameter optimisation and reproduce the temperature programmed desorption (TPD) of CO from Rh(100) as well.[51] The current model, combined with desorption activation energies $E_{\mathrm{des,top}} = 126$ kJ mol^{-1}, $E_{\mathrm{des,bridge}} = 120$ kJ mol^{-1} and a prefactor of $\nu = 10^{12}$ s^{-1} already gives a very reasonable description.

Infared (IR) intensity measurements can be taken as a qualitative measure for the distribution of CO molecules over top and bridge sites. This is done by comparing the IR intentsity of the vibrational band associated with bridge bound CO, with the intensity of the vibrational band associated with top bound CO.[4,12,47] The general trend described by Leung*et al*., who report over the largest coverage interval, is that up to 0.50 ML top occupation dominates. Above 0.50 ML the intensity of the peak associated with top bound CO strongly decreases, while the intensity of the peak associated with bridge bound CO strongly increases. This supports the idea of the formation of a $(4\sqrt{2} \times \sqrt{2})$ structure with a majority of CO molecules in bridge sites. At increasing coverage, the intensity of the peak associated with top bound CO increases again, while the intensity of the peak associated with bridge bound CO becomes smaller. All these features are reproduced by our model, see Fig. 7, bottom panel. The distribution of CO over top and bridge sites has also been studied by different techniques. For the case of the $(4\sqrt{2} \times \sqrt{2})$ structure, it was shown by means of high resolution photoelectron spectroscopy (PES) and X-ray photoelectron spectroscopy (XPS) that there are twice as many CO molecules in bridge sites than there are in top sites.[5,52]

Comparing the parameters for Pt(100) with the ones for Rh(100), one notes the following changes. The increase in φ_3(t–t) destabilises the c(4 × 2)−4t + 2b structure with respect to the c(4 × 2)−2t + 4b and $(4\sqrt{2} \times \sqrt{2})$ structure at 0.75 ML coverage. The increase in φ_4 stabilises the $(4\sqrt{2} \times \sqrt{2})$ structure with respect to the c(4 × 2)−2t + 4b ordered structure. The increase in φ_4 also destabilises the $(3\sqrt{2} \times \sqrt{2})$ structure to such an extent that it is not observed anymore at 0.67 ML coverage.

4.3 General comparison

Mason *et al*. have performed DFT calculations within the GGA approximation of CO on Pt(100) and Rh(100) from which estimates of lateral interactions were derived.[19] In this work it is concluded that for both the Rh(100) surface and the Pt(100) surface the difference in binding energy between top and bridge site is small, in agreement with the experimental observation of adsorption on both types of sites. They show that the φ_3 interactions according to their calculation strategy are in the range of 18–32 kJ mol^{-1}, while interactions at a larger distance than φ_4 are less than 6 kJ mol^{-1}. The interaction φ_4 itself was not determined. These data support the choice of our model, where the interactions φ_3 and φ_4 are taken into account, while interactions at a larger distance are ignored. In terms of the absolute size of the interactions, one can say the following. Our interactions form a lower limit, since we determine the minimum value of the interaction that is needed to create an ordered structure. Our lower limit estimates are 5–13 kJ mol^{-1} ($4k_{\mathrm{B}}T$–$10k_{\mathrm{B}}T$ at 150 K) for the φ_3 interactions, which is in good agreement with the DFT estimates of the actual values of 18–32 kJ mol^{-1}.

An earlier study by Eichler *et al*. of CO adsorption on Rh(100) yielded different results. In that study it was found that there was less than 10 kJ mol^{-1} difference between a p(2 × 2), a p(2 ×1) and a c(2 × 2) ordered structure, both for top and bridge site adsorption. This implies that φ_3 must be substantially smaller than the 18–32 kJ mol^{-1} found by Mason *et al*.[18] This study also reports adsorption energy values for 0.75 ML and 1.00 ML coverage, and from those values it is clear that at higher coverages (larger than 0.50 ML) lateral interactions do after all reduce the adsorption energy. This study indicates an energetic preference for the bridge site at low coverage, but tries to reconcile this with the experimental observation of combined top/bridge adsorption by assuming that the adsorption mechanism steers the CO molecules towards the top sites. An alternative explanation, also provided by the authors, is a failure of the density-functional theory to accurately describe this case. A similar strong and unexpected preference for the bridge site was published by the same authors for CO on Pt(100).[53]

The interaction described in Fig. 2 probably also plays a role in the ordering behaviour of bridge bonded CO on other transition metal surfaces. CO is known to adsorb on bridge sites on Pd(100), and both on top and bridge sites on Ni(100). The ordered structures of CO on Pd(100) show a tendency to avoid the adsorption of three or more CO molecules right next to each other.[8,9,54,55] This is only possible up to a total coverage of 0.67 ML. A similar tendency is seen for the ordered structures of CO on Ni(100).[8,9] It is important to mention here that even though in our model the interaction is

modelled as infinitely repulsive, this need not be the case in practice. A significant interaction of several times the thermal energy is enough to give similar results to the ones presented here. The c(6 × 2) ordered structure is not found in our simulations when the interaction described in Fig. 2 is not applied in our model.

In two cases we find an ordered structure which is different from the one proposed in the literature: the $(3\sqrt{2} \times \sqrt{2})$ structure at 0.67 ML coverage on Pt(100), and the $(4\sqrt{2} \times \sqrt{2})$ structure at 0.75 ML coverage on Rh(100). In both cases, we can see a different distribution of adsorbates inside the unit cell. This different distribution inside the unit cell causes the unit cell to simplify from a $(4\sqrt{2} \times \sqrt{2})$ unit cell into a $(2\sqrt{2} \times \sqrt{2})$ unit cell for the Rh(100) case. The experimentally observed structure is in both cases, according to our interaction rules, equal in energy to the one found in our simulations. The reason why we do find those particular structures in our model, is the one-dimensional ordering, which gives a slight entropic advantage over the experimentally observed structures. The experimentally proposed structures have a different advantage, however. These structures can both relax into a pseudo-hexagonal arrangement, thus maximising the mutual adsorbate–adsorbate distance. Assuming a dipole–dipole interaction through space repulsion between the adsorbates in addition to the through surface interactions used in our model, and allowing some spatial relaxation, one would thus expect our one-dimensionally ordered structures to convert into the pseudo-hexagonal arrangements proposed based on the experiments.

The inclusion of additional pair interactions, without allowing the adsorbates to relax from their ideal positions, does not promote the formation of the $(3\sqrt{2} \times \sqrt{2})$ ordered structure at the expense of the one-dimensionally ordered structure. More (three- or four-) particle interactions are smaller than pair interactions, so these will probably not produce only a $(3\sqrt{2} \times \sqrt{2})$ ordered structure either, without the presence of the one-dimensionally ordered phase.[20]

Both the models for CO on Pt(100) and Rh(100) allow adsorption up to a total coverage of 1.00 ML. Under experimental conditions, the saturation coverage is lower, 0.83 ML. This difference in saturation coverage is due to the continuous increase in simulated pressure in the model *versus* the constant pressure adsorption used in the experiments.

Finally, it is interesting to remark on the possibility of off-lattice or incommensurate adsorption of CO. The results of the current model indicate that a lot of the features of the adsorption behaviour of CO can be reproduced by a lattice model. However, the differences with experimental findings indicate that some relaxation away from the ideal position may take place in practice. We, however, do not see any indication that true incommensurate adsorption takes place at high coverage. Multilayer adsorption has been reported for CO on Ni(100) and Cu(100). The presence of multilayer adsorption does not strongly influence the adlayer ordering as described in this article.[56,57]

5. Conclusions

We have developed a lattice gas Monte Carlo model with lateral interactions between the adsorbates that describes the high (and low) coverage ordering behaviour of CO on the Rh(100) and the Pt(100) surface. The model includes bridge and top site adsorption, desorption, diffusion, and pairwise lateral interactions between the adsorbates. One additional interaction is taken into account: a CO molecule is forbidden to adsorb on a bridge site formed by two surface atoms when both surface atoms are already forming a bond with other CO molecules. This exclusion is based on bond order conservation principles, and plays a crucial role in the ordering behaviour of CO at high coverages.

For CO on Pt(100), the c(2 × 2)−2t structure at 0.50 ML, a structure similar to the $(3\sqrt{2} \times \sqrt{2}) - 2t + 2b$ structure at 0.67 ML, the c(4 × 2)−4t + 2b structure at 0.75 ML, and the recently reported c(6 × 2) structure at 0.83 ML were reproduced by our model. The experimentally reported $(5\sqrt{2} \times \sqrt{2})$ structure at 0.60 ML was not reproduced by our model. Our model, similar to the STM measurements by Wakisaka, favours the formation of a c(4 × 2)−4t + 2b structure at 0.75 ML, making the alternative c(4 × 2)−2t + 4b structure less likely. The difference in the observed structures at 0.67 ML coverage is explained by the assumption that in the experiment the adsorbates can relax into a pseudo-hexagonal arrangement, which cannot be reproduced by the lattice model described here.

For CO on Rh(100), the c(2 × 2)−2t structure at 0.50 ML, a structure similar to the $(4\sqrt{2} \times \sqrt{2}) - 2t + 4b$ structure at 0.75 ML, and the c(6 × 2) structure at 0.83 ML were reproduced by our model. The distribution of adsorbates over top and bridge sites as a function of coverage was also compared to IR measurements, and found to match the experimental observations. The difference in observed structure at 0.75 ML coverage is explained by the assumption that in the experiment the adsorbates can relax into a pseudo-hexagonal arrangement, which cannot be reproduced by the lattice model described here.

This is the first Monte Carlo model able to accurately describe the high coverage ordering behaviour of CO on fcc(100) surfaces. The success of this model indicates that the lattice gas approximation remains useful for modelling the adsorption behaviour of CO on transition metal surfaces up to the highest achievable (saturation) coverage.

References

1 I. Zasada, M. A. van Hove and G. A. Somorjai, *Surf. Sci.*, 1998, **418**, L89–L93.
2 N. Materer, A. Barbieri, D. Gardin, U. Starke, J. D. Batteas, M. A. van Hove and G. A. Somorjai, *Phys. Rev. B: Condens. Matter*, 1993, **48**, 2859–2861.
3 N. Materer, A. Barbieri, D. Gardin, U. Starke, J. D. Batteas, M. A. van Hove and G. A. Somorjai, *Surf. Sci.*, 1994, **303**, 319–332.
4 L.-W. H. Leung, J.-W. He and D. W. Goodman, *J. Chem. Phys.*, 1990, **93**, 8328–8336.
5 F. Strisland, A. Ramstadt, T. Ramsvik and A. Borg, *Surf. Sci.*, 1998, **415**, L1020–L1026.
6 S. Aminpirooz, A. Schmalz, L. Becker and J. Haase, *Phys. Rev. B: Condens. Matter*, 1992, **45**, 6337–6340.
7 D. G. Castner, B. A. Sexton and G. A. Somorjai, *Surf. Sci.*, 1978, **71**, 519–540.
8 J. P. Biberian, *Surf. Sci.*, 1982, **118**, 443–464.
9 P. Uvdal, P.-A. Karlsson, C. Nyberg, S. Andersson and N. V. Richardson, *Surf. Sci.*, 1988, **202**, 167–182.

10 C. W. Tucker, *J. Appl. Phys.*, 1966, **37**, 3013–3019.
11 G. Brodén, G. Pirug and H. P. Bonzel, *Surf. Sci.*, 1978, **72**, 45–52.
12 B. A. Gurney, L. J. Richter, J. S. Villarubia and W. Ho, *J. Chem. Phys.*, 1987, **87**, 6710–6721.
13 C. G. M. Hermse, *An overview of ordered adlayer structures for CO and NO on the (100) surface of Pt, Rh, Ni, Cu and Pd*, 2009, arXiv:0906.2333v1.
14 C. Popa, C. F. J. Flipse, A. P. J. Jansen, R. A. van Santen and P. Sautet, *Phys. Rev. B: Condens. Matter Mater. Phys.*, 2006, **73**, 245408 (10 pages).
15 M. Wakisaka, T. Ohkanda, T. Yoneyama, H. Uchida and M. Watanabe, *Chem. Commun.*, 2005, 2710–2712.
16 P. J. Feibelman, B. Hammer, J. K. Nørskov, F. Wagner, R. Stumpf, R. Watwe and J. Dumesic, *J. Phys. Chem. B*, 2001, **105**, 4018–4025.
17 B. Hammer, L. B. Hansen and J. Nørskov, *Phys. Rev. B: Condens. Matter Mater. Phys.*, 1999, **59**, 7413–7421.
18 A. Eichler and J. Hafner, *J. Chem. Phys.*, 1998, **109**, 5585–5595.
19 S. E. Mason, I. Grinberg and A. M. Rappe, *J. Phys. Chem. B*, 2006, **110**, 3816–3822.
20 A. P. J. Jansen and C. Popa, *Phys. Rev. B: Condens. Matter Mater. Phys.*, 2008, **78**, 085404, 9 pages.
21 Y. Zhang, V. Blum and K. Reuter, *Phys. Rev. B: Condens. Matter Mater. Phys.*, 2007, **75**, 235406 (14 pages).
22 A. B. Mhadeshwar, J. R. Kitchin, M. A. Barteau and D. G. Vlachos, *Catal. Lett.*, 2004, **96**, 13–22.
23 S. D. Miller and J. R. Kitchin, *Surf. Sci.*, 2009, **603**, 794–801.
24 B. N. J. Persson, *Surf. Sci. Rep.*, 1992, **15**, 1–135.
25 A. Patrykiejew, S. Sokolowski and K. Binder, *Surf. Sci. Rep.*, 2000, **37**, 207–344.
26 M. T. M. Koper and J. J. Lukkien, *Surf. Sci.*, 2002, **498**, 105–115.
27 C. G. M. Hermse, A. P. van Bavel, M. T. M. Koper, J. J. Lukkien, R. A. van Santen and A. P. J. Jansen, *Phys. Rev. B: Condens. Matter Mater. Phys.*, 2006, **73**, 195422 (9 pages).
28 D.-J. Liu, *J. Chem. Phys.*, 2004, **121**, 4352–4357.
29 D.-J. Liu and J. W. Evans, *Phys. Rev. B: Condens. Matter Mater. Phys.*, 2004, **70**, 193408.
30 A. P. J. Jansen, *Phys. Rev. B: Condens. Matter Mater. Phys.*, 2004, **69**, 035414 (6 pages).
31 R. Kose, W. A. Brown and D. A. King, *J. Phys. Chem. B*, 1999, **103**, 8722–8725.
32 Y. Y. Yeo, L. Vattuone and D. King, *J. Chem. Phys.*, 1996, **104**, 3810–3821.
33 V. P. Zhdanov and P. R. Norton, *Surf. Sci.*, 1994, **312**, 441–449.
34 V. P. Zhdanov and P. R. Norton, *Surf. Sci.*, 1996, **350**, 271–276.
35 D.-J. Liu and J. W. Evans, *J. Chem. Phys.*, 2006, **124**, 154705.
36 D.-J. Liu, *J. Phys. Chem. C*, 2007, **111**, 14698–14706.
37 B. N. J. Persson, *J. Chem. Phys.*, 1990, **92**, 5034–5046.
38 B. N. J. Persson, *Surf. Sci.*, 1991, **258**, 451–463.
39 C. G. M. Hermse and A. P. J. Jansen, in *Catalysis*, The Royal Society of Chemistry, 2006, vol. 19, ch., Kinetics of Surface Reactions with Lateral Interactions: Theory and Simulations, pp. 109–164.
40 J. J. Lukkien, J. P. L. Segers, P. A. J. Hilbers, R. J. Gelten and A. P. J. Jansen, *Phys. Rev. E: Stat. Phys., Plasmas, Fluids, Relat. Interdiscip. Top.*, 1998, **58**, 2598–2610.
41 A. P. J. Jansen, *Comput. Phys. Commun.*, 1995, **86**, 1–12.
42 P. van Beurden, *PhD thesis*, Eindhoven University of Technology, 2003.
43 R. Martin, P. Gardner and A. M. Bradshaw, *Surf. Sci.*, 1995, **342**, 69–84.
44 M.-B. Song, K. Yoshimi and M. Ito, *Chem. Phys. Lett.*, 1996, **263**, 585–590.
45 C. K. Rhee, J. M. Feliu, E. Herrero, P. Mrozek and A. Wieckowski, *J. Phys. Chem.*, 1993, **97**, 9730–9735.
46 A. M. de Jong, *PhD thesis*, Eindhoven University of Technology, 1994.
47 A. M. de Jong and J. W. Niemantsverdriet, *J. Chem. Phys.*, 1994, **101**, 10126–10133.
48 A. P. van Bavel, *PhD thesis*, Eindhoven University of Technology, 2005.
49 L. J. Richter, B. A. Gurney and W. Ho, *J. Chem. Phys.*, 1987, **86**, 477–490.
50 Y. Kim, H. C. Peebles and J. M. White, *Surf. Sci.*, 1982, **114**, 363–380.
51 M. M. M. Jansen, unpublished work.
52 A. Baraldi, L. Gregoratti, G. Cornelli, V. R. Dhanak, M. Kiskinova and R. Rosei, *Appl. Surf. Sci.*, 1996, **99**, 1–8.
53 A. Eichler and J. Hafner, *J. Catal.*, 2001, **204**, 118–128.
54 J. N. Andersen, M. Qvarford, R. Nyholm, S. L. Sorensen and C. Wigren, *Phys. Rev. Lett.*, 1991, **67**, 2822–2825.
55 W. Berndt and A. M. Bradshaw, *Surf. Sci.*, 1992, **279**, L165–L169.
56 J. C. Cook and E. M. McCash, *Surf. Sci.*, 1996, **356**, L445–L449.
57 V. Formoso, A. Marino, G. Chiarello, R. G. Agostino, T. Caruso and E. Colavita, *Surf. Sci.*, 2006, **600**, 1456–1461.